Published in final edited form as:
Neurotoxicology. 2006 March ; 27(2): 237–244. doi:10.1016/j.neuro.2005.10.004.

Molecular basis of differential sensitivity of insect sodium channels to DCJW, a bioactive metabolite of the oxadiazine insecticide indoxacarb

Weizhong Song, **Zhiqi Liu**, and **Ke Dong***
Department of Entomology and Neuroscience Program, Michigan State University, East Lansing, MI 48824, USA

Abstract

Indoxacarb (DPX-JW062) was recently developed as a new oxadiazine insecticide with high insecticidal activity and low mammalian toxicity. Previous studies showed that indoxacarb and its bioactive metabolite, *N*-decarbomethoxyllated JW062 (DCJW), block insect sodium channels in nerve preparations and isolated neurons. However, the molecular mechanism of indoxacarb/DCJW action on insect sodium channels is not well understood. In this study, we identified two cockroach sodium channel variants, $BgNa_v1$-1 and $BgNa_v1$-4, which differ in voltage dependence of fast and slow inactivation, and channel sensitivity to DCJW. The voltage dependence of fast inactivation and slow inactivation of $BgNa_v1$-4 were shifted in the hyperpolarizing direction compared with those of $BgNa_v1$-1 channels. At the holding potential of −90 mV, 20 μM of DCJW reduced the peak current of $BgNa_v1$-4 by about 40%, but had no effect on $BgNa_v1$-1. However, at the holding potential of −60 mV, DCJW also reduced the peak currents of $BgNa_v1$-1 by about 50%. Furthermore, DCJW delayed the recovery from slow inactivation of both variants. Substitution of E1689 in segment 4 of domain four (IVS4) of $BgNa_v1$-4 with a K, which is present in $BgNa_v1$-1, was sufficient to shift the voltage dependence of fast and slow inactivation of $BgNa_v1$-4 channels to the more depolarizing membrane potential close to that of $BgNa_v1$-1 channels. The E1689K change also eliminated the DCJW inhibition of $BgNa_v1$-4 at the hyperpolarizing holding potentials. These results show that the E1689K change is responsible for the difference in channel gating and sensitivity to DCJW between $BgNa_v1$-4 and $BgNa_v1$-1. Our results support the notion that DCJW preferably acts on the inactivated state of the sodium channel and demonstrate that K1689E is a major molecular determinant of the voltage-dependent inactivation and state-dependent action of DCJW.

Keywords

Insect sodium channel; Insecticide; Indoxacarb; DCJW; *Xenopus* oocyte

1. Introduction

Voltage-gated sodium channels are responsible for the generation of action potentials across the membranes of excitable cells. They are the primary targets of natural neurotoxins such as tetrodotoxin from the puffer fish, therapeutic drugs such as local anesthetics, and several important classes of synthetic insecticides including pyrethroids and the oxadiazine

* Corresponding author. Tel.: +1 517 432 2034; fax: +1 517 353 5598. dongk@msu.edu (K. Dong)..

insecticide indoxacarb. Pyrethroid insecticides are synthetic derivatives of the naturally occurring pyrethrum extract from chrysanthemum plants, and, in the past several decades, have played a prominent role in the control of insect pests of agricultural or medical importance. Intensive use of pyrethroids in pest control, however, has led to the development of pyrethroid resistance in many pest populations. Indoxacarb (DPX-JW062) is a new insecticide that possesses high insecticidal activity and low mammalian toxicity (Wing et al., 1998, 2000, 2004). In insects, indoxacarb is metabolically converted to *N*-decarbomethoxyllated JW062 (DCJW), which is more active than its parental compound (Wing et al., 1998, 2000). Indoxacarb is now considered to be a promising alternative to pyrethroid insecticides, especially for the control of lepidopterous pests of agricultural importance (Wing et al., 1998, 2000).

Like their mammalian counterparts, sodium channel proteins in insects contain four homologous domains (I–IV), each having six transmembrane segments (S1–S6) (Loughney et al., 1989). The structural features that are critical for mammalian sodium channel function are also conserved in insect sodium channels. Upon membrane depolarization, voltage-gated sodium channels open (activate), initiated by the outward movement of the S4 segments, which function as voltage sensors, through the electric field across the membrane (refs. in Catterall, 2000). The location of the activation gate and the mechanism of the coupling between the voltage sensors and the gate are still not completely understood. A few milliseconds after channel opening, sodium channels rapidly inactivate (known as fast inactivation). Fast inactivation is mediated by an inactivation gate, which is composed of residues in the third linker connecting the domains III and IV (Catterall, 2000). Fast inactivation occurs within milliseconds of membrane depolarization and plays an important role in the termination of action potentials. In response to prolonged depolarization on a time scale of seconds to minutes, however, sodium channels progressively enter into more stable, slow-inactivated states that are kinetically and molecularly distinct from fast inactivation (Rudy, 1978; Schauf et al., 1976; Wang and Wang, 1997; O'Reilly et al., 2001). These non-conducting states have diverse lifetimes ranging from seconds to minutes, and are distinct from fast inactivated states, which typically have lifetime less than 10 ms. Although little is known about the molecular determinants of slow inactivation, it is believed to be important in regulating membrane excitability, action potential firing patterns, and spike frequency adaptation (Simoncini and Stuűhmer, 1987; Ruff et al., 1988; Hayward et al., 1997).

The mechanism of pyrethroid action on sodium channels has been a subject of study for decades and is now well-established (refs. in Narahashi, 2000; refs. in Soderlund and Knipple, 2003). However, studies on the mechanism of action of indoxacarb/DCJW on sodium channels are limited (refs. in Wing et al., 2004; Silver and Soderlund, 2005a). Indoxacarb and DCJW were found to block sodium-dependent compound action potentials in extracellular recordings of nerve cord preparations from tobacco budworm (*Manduca sexta*) larvae (Wing et al., 1998, 2000). A subsequent study involving whole-cell sodium current recorded from dorsal unpaired median (DUM) neurons of the cockroach *Periplaneta americana* further confirmed that DCJW blocks sodium channels in a dose-dependent manner (Lapied et al., 2001). The blocking effect of indoxacarb/DCJW on tetrodotoxin (TTX)-sensitive and TTX-resistant mammalian sodium channels was also reported in dorsal root ganglion neurons (Nagata et al., 1998; Zhao et al., 2003). Interestingly, TTX-sensitive sodium currents were more sensitive to inhibition by DCJW than were TTX-resistant sodium channels, possibly due to a more negative voltage-dependence of steady-state inactivation of TTX-sensitive sodium channels (Zhao et al., 2003).

In this study, we examined the effects of DCJW on cockroach sodium channel ($BgNa_V$) splice variants expressed in *Xenopus* oocytes. We identified two cockroach sodium channel variants that exhibited distinct gating properties and differential sensitivity to DCJW.

Further experiments uncovered an amino acid residue, E1689, that is responsible for the variant-specific response. While this manuscript was ready for submission, two independent studies on DCJW were reported by Silver and Soderlund (2005b) and Zhao et al. (2005). Zhao et al. (2005) found that two types of TTX-sensitive sodium currents in cockroach neurons possessed distinct voltage-dependence of inactivation and exhibited differential responses to indoxacarb/DCJW, suggesting state-dependence of the DCJW blocking effect. Silver and Soderlund (2005b) documented similar state-dependent DCJW inhibition of mammalian $Na_v1.4$ channels expressed in *Xenopus* oocytes. Our results support the idea that DCJW preferentially interacts with the inactivated state of the sodium channel and revealed the first amino acid, K1689E, in the sodium channel that plays a critical role in both the voltage-dependent inactivation of the sodium channel and the state-dependent action of DCJW.

2. Materials and methods

2.1. Construction of a recombinant $BgNa_v$ channel

In a previous study, we isolated 69 $BgNa_v$ full-length cDNA clones, which were grouped into 20 splice types (Tan et al., 2002; Song et al., 2004). Eleven variants were functionally characterized and three of them, $BgNa_v1$-1, -2, and -3, belong to splice type 1 (Tan et al., 2002; Song et al., 2004). $BgNa_v1$-4, a fourth variant belonging to splice type 1, was expressed and functionally characterized in this study. The $BgNa_v1\text{-}4^{E1689K}$ recombinant channel was constructed by excising an Eco47III fragment (1429 bp) containing K1689, from $BgNa_v1$-1variant and subcloning the fragment into $BgNa_v1$-4 to replace the corresponding fragment carrying E1689 in $BgNa_v1$-4.

2.2. Expression of $BgNa_v$ sodium channels in Xenopus oocytes

The procedures for oocyte preparation and cRNA injection are identical to those described by Tan et al. (2002). For robust expression of the cockroach $BgNa_v$ sodium channels, $BgNa_v$ cRNA was coinjected into oocytes with cRNA of the auxiliary subunit of *D. melanogaster* sodium channels (tipE), which is known to enhance the expression of insect sodium channels in oocytes (Feng et al., 1995; Warmke et al., 1997).

2.3. Two-electrode voltage-clamp recording from oocytes

All oocyte recordings were performed at room temperature (20–22 °C) in ND96 bath solution (96.0 mM NaCl; 2.0 mM KCl; 1.8 mM $CaCl_2$; 1.0 mM $MgCl_2$; 10.0 mM HEPES, adjust pH to 7.5 with 2 N NaOH). Recording electrodes were prepared from borosilicate glass using a P-87 puller (Sutter Instrument Co., Novato, CA). Microelectrodes were filled with filtered 3 M KCl/0.5% agarose and had a resistance between 0.4 and 1.0 MΩ. Currents were recorded and analyzed using the oocyte clamp instrument OC725C (Warner Instrument Corp., Hamden, CT), Digidata 1322A interface (Axon Instrument, Union, CA), and pClamp 8.0 software (Axon instruments, Union, CA). Data were filtered at 2 kHz on-line and digitized at a sampling frequency of 20 kHz. Capacitance transients and leak currents were corrected by P/4 subtraction, except for the recovery from inactivation.

2.4. Toxins and toxin application

DCJW and indoxacarb were gifts from Dupont company. They were dissolved in DMSO as 10 mM stock solution and kept at −20 °C. The working concentration was prepared in ND96 recording solution immediately prior to experiments. The concentration of DMSO in the final solution was <0.5% (v/v), which had no effect on sodium channels in our experimental conditions. The method for application of the toxins was identical to that described in Tan et al. (2002).

2.5. Data analysis

Data were expressed as mean ± S.D. from at least four oocytes. Statistical comparisons were performed using unpaired Student's *t*-test with $p < 0.05$ considered statistically significant.

3. Results

3.1. Sodium channel variants respond to DCJW differently

In an earlier study, we identified 20 splice types of the cockroach sodium channel gene, $BgNa_v$, which differ in the alternative exon usage (Song et al., 2004). Functional characterization of these splice variants expressed in oocytes revealed substantial differences in gating properties (Tan et al., 2002; Song et al., 2004; Liu et al., 2004). In this study we examined the effect of DCJW on 18 previously characterized splice variants, which include $BgNa_v1$-1 (denoted as the first variant of splice type 1), $BgNa_v1$-2, $BgNa_v4$, $BgNa_v5$, $BgNa_v6$, $BgNa_v7$, $BgNa_v8$, $BgNa_v9$, and $BgNa_v10$ (Song et al., 2004), and nine new variants (named $BgNa_v1$-4 to $BgNa_v1$-12) of splice type 1. From the holding potential of −90 mV, peak sodium current was elicited by a 20 ms test pulse to −10 mV. The peak current was recorded every 3 min to ensure no inactivation accumulated. DCJW was applied only after the peak current reached a stable level. DCJW had no inhibitory effects on the peak current of $BgNa_v1$-1 or any of the other 16 variants, except for $BgNa_v1$-4. $BgNa_v1$-4 exhibited sensitivity to inhibition of peak current by DCJW under these conditions. DCJW (20 μM) inhibited peak current of $BgNa_v1$-4 by about 40% (Fig. 1A). For $BgNa_v1$-4, the DCJW inhibition did not reach a plateau even 1 h after toxin application although significant inhibition was achieved in 30 min (Fig. 1B), suggesting that DCJW is a slow-acting toxin. $BgNa_v1$-4 has six unique amino acid residues: V55G (e.g., G in $BgNa_v1$-4 and V in other variants), L993F, D1145G, I1663M, K1689E and D1849N. I1663M is the result of an A-to-I editing (Song et al., 2004), whereas the causes of the other amino acid changes remain to be determined.

3.2. DCJW inhibition of sodium currents is greater at more depolarizing holding potentials

To investigate the underlying mechanism of the different sensitivities of variants $BgNa_v1$-1 and $BgNa_v1$-4 to DCJW, we examined the DCJW inhibition of peak sodium current at various holding potentials (Fig. 2). Peak currents were evoked by a 20 ms depolarization to −10 mV. In the drug-free condition, depolarization to −10 mV from the holding potential of −120 mV produced the maximal peak current in both $BgNa_v1$-1 and $BgNa_v1$-4 channels indicating that nearly all $BgNa_v1$-1 and $BgNa_v1$-4 channels were in the resting state. Peak currents recorded at other holding potentials were normalized to the peak current obtained at −120 mV. At more positive membrane potentials, such as −90 mV, a portion of $BgNa_v1$-4 channels were inactivated, but $BgNa_v1$-1 channels remained in the resting state (Fig. 2). When the holding potential was maintained at −70 mV, about 80% of $BgNa_v1$-4 channels were in the inactivated state, compared to only about 10% of $BgNa_v1$-1 channels (Fig. 2). Thus, compared with $BgNa_v1$-1, $BgNa_v1$-4 channels enter into the inactivated state at more negative holding potential.

To examine whether the differential effects of DCJW on $BgNa_v1$-1 and $BgNa_v1$-4 channels is correlated with the difference in availability of inactivated channels, we examined the DCJW effect on $BgNa_v1$-1 and $BgNa_v1$-4 at different holding potentials. DCJW was applied after the peak current reached a stable level, and the DCJW inhibition of peak current was measured after 30 min of DCJW treatment. At the holding potential of −120 mV, DCJW did not reduce the amplitude of peak current of either $BgNa_v1$-1 or $BgNa_v1$-4 channels (Fig. 2), indicating that DCJW had no effect on sodium channels in the resting state. At the holding potential of −90 mV, DCJW reduced the amplitude of peak current of $BgNa_v1$-4 by 41%, but had no affect on $BgNa_v1$-1 (Fig. 2). At −70 mV, DCJW inhibited 13% and 81% of the

peak currents of $BgNa_v1$-1 and $BgNa_v1$-4, respectively (Fig. 2). Clearly, for both channel variants greater DCJW inhibition was observed when the proportion of inactivated channels increased.

3.3. DCJW slows the recovery from slow inactivation

To gain a more detailed understanding of the effects of DCJW, we examined the effects of DCJW on the gating properties of $BgNa_v1$-1 and $BgNa_v1$-4. $BgNa_v1$-1 was functionally characterized in an earlier study (Tan et al., 2002; Song et al., 2004), whereas the $BgNa_v1$-4 channel has not. We found that the $BgNa_v1$-4 channel activated and inactivated rapidly with the gating kinetics similar to those of $BgNa_v1$-1 (data not shown). $BgNa_v1$-4 was also sensitive to TTX, being completely blocked by 20 nM TTX (data not shown). However, the voltage-dependence of activation, steady-state fast inactivation, and slow inactivation of $BgNa_v1$-4 was shifted in the hyperpolarizing direction by 6, 25, and 16 mV, respectively, compared with $BgNa_v1$-1 (Fig. 3A–C, Table 1). The recovery from fast inactivation of $BgNa_v1$-4 was much slower than that of $BgNa_v1$-1 (Fig. 3D), with time constant of 8.5 ms compared with 2.5 ms for $BgNa_v1$-1.

DCJW had no observable effect on the voltage-dependence of activation or fast inactivation of $BgNa_v1$-4 and $BgNa_v1$-1 channels (data not shown). Although recovery from fast inactivation of $BgNa_v1$-4 was inherently much slower than that of $BgNa_v1$-1, DCJW did not change the kinetics of recovery from fast inactivation of either $BgNa_v1$-4 or $BgNa_v1$-1 (Fig. 4A and B). We also did not observe any use-dependent block of DCJW. Delivering 50 depolarizing pulses to −10 mV at 20 Hz did not cause any change in peak current in the presence of DCJW (data not shown). The only significant effects of DCJW were on slow inactivation. DCJW slowed the rate of recovery from slow inactivation for both $BgNa_v1$-1 and $BgNa_v1$-4 channels (Fig. 4C and D).

3.4. K1689E is responsible for the differences in voltage-dependent channel inactivation and DCJW sensitivity between $BgNa_v1$-1 and $BgNa_v1$-4

To determine which amino acid residue(s) in $BgNa_v1$-4 is responsible for the unique gating properties and DCJW sensitivity of $BgNa_v1$-4, we compared the amino acid sequences of $BgNa_v1$-1 and $BgNa_v1$-4. Although $BgNa_v1$-4 has the same alternative exon usage as $BgNa_v1$-1, it has six unique amino acid residues: V55G (V in $BgNa_v1$-1 and G in $BgNa_v1$-4), L993F, D1145G, I1663M, K1689E and D1849N. K1689E is particularly intriguing because K is one of the positively charged residues in IVS4 that is critical for voltage-dependent gating. We therefore hypothesized that the K to E change at this position could alter channel gating. To test this hypothesis, we replaced E with K and examined the gating properties of the resulting recombinant $BgNa_v1$-4^{E1689K} channel. We found that the activation of the $BgNa_v1$-4^{E1689K} channel was not significantly different from that of $BgNa_v1$-4, except for a steeper voltage-dependence (Fig. 5A, Table 1). However, the voltage-dependence of fast and slow inactivation of the $BgNa_v1$-4^{E1689K} channel were shifted to more positive membrane potentials compared with $BgNa_v1$-4, and were similar to those of $BgNa_v1$-1 (Fig. 5B and C). In addition, the recovery from fast inactivation of the $BgNa_v1$-4^{E1689K} channel is similar to that of $BgNa_v1$-1 channel (Fig. 5D). Thus, the amino acid residue E1689 is responsible for the unique voltage-dependence of fast inactivation and slow inactivation in $BgNa_v1$-4.

To determine whether the E1689K substitution also alters the sensitivity of the $BgNa_v1$-4 channel to DCJW, we examined the DCJW effect on the $BgNa_v1$-4^{E1689K} channel. At the holding potential of −90 mV, DCJW did not reduce the peak current of the $BgNa_v1$-4^{E1689K} channel (Fig. 6A). However, at the holding potential of −60 mV, DCJW inhibited the peak current by 50% (Fig. 6A). Overall, the response of the $BgNa_v1$-4^{E1689K} channel to DCJW

was strikingly similar to that of the $BgNa_v1$-1 channel (Fig. 6B). These results demonstrate that a single amino acid residue determines differential voltage-dependence of inactivation and DCJW sensitivity between $BgNa_v1$-1 and $BgNa_v1$-4.

We also determined the apparent dissociation constants (K_I) of DCJW for the inactivated state of $BgNa_v1$-1 and $BgNa_v1$-4 channels. K_I for inactivated state was determined according to the equation $K_I = (1 - h)(1/I_D - 1)[D]$, where h is the fraction of inactivated channels in control, and I_D is the fraction of channels blocked at the drug concentration [D] (Kuo and Bean, 1994; Yarov-Yarovoy et al., 2001). The holding potential of −90 mV was used for $BgNa_v1$-4, and −60 mV for both $BgNa_v1$-1 and $BgNa_v1$-4^{E1689K} channels. We did not observe any significant difference in K_I among the three channels ($p > 0.05$): 2.3 μM for $BgNa_v1$-1, 2.4 μM for $BgNa_v1$-4 and 2.6 μM for $BgNa_v1$-4^{E1689K}. These results further confirmed that the differential responses of $BgNa_v1$-1 and $BgNa_v1$-4 channels to DCJW are the results of the differences in channel gating, not in DCJW binding to its receptor site.

4. Discussion

In this study, we determined the effects of the bioactive metabolite, DCJW, of a new insecticide indoxacarb on cockroach sodium channels expressed in *Xenopus* oocytes. In addition to providing an independent confirmation of the sodium channel-blocking effect of DCJW, our results presented in Fig. 2 suggest that DCJW preferentially binds to the inactivated state, but not to the resting state of the sodium channel. Moreover, we discovered that two cockroach sodium channel variants, $BgNa_v1$-1 and $BgNa_v1$-4, exhibited different gating properties and differential sensitivities to DCJW. $BgNa_v1$-1 is a previously characterized cockroach sodium channel variant (Tan et al., 2002), whereas $BgNa_v1$-4 is a new variant functionally characterized in this study. By studying the amino acid differences between $BgNa_v1$-1 and $BgNa_v1$-4, we identified the first amino acid (K1689E in IVS4 of the sodium channel) that is responsible for both the enhanced sensitivity of $BgNa_v1$-4 to DCJW and a large negative shift of this variant's voltage-dependence of steady-state inactivation. The demonstrated involvement of E1689K in the coupling of voltage-dependence of channel inactivation and DCJW sensitivity provides the first molecular insight into the state-dependent action of DCJW on the sodium channel. We further showed that the K1698E change did not alter DCJW binding to the channels and that upon binding, DCJW stabilizes the slow-inactivated state of sodium channels. Whether the K1689E change in $BgNa_v1$-4 is the result of RNA editing remains to be determined.

The state-dependent action of DCJW on insect sodium channels expressed in oocytes in this study is in good agreement with other studies using mammalian and insect neurons or mammalian sodium channels expressed in oocytes. For example, TTX-sensitive sodium currents in DRG neurons were more sensitive to inhibition by DCJW than were TTX-resistant sodium channels, possibly due to a more negative voltage-dependence of steady-state inactivation of TTX-sensitive sodium channels (Zhao et al., 2003). Two types of sodium currents were detected in dissociated cockroach neurons (Zhao et al., 2003). These two sodium currents possessed distinct voltage-dependence of inactivation and exhibited differential responses to indoxacarb/DCJW (Zhao et al., 2003). Finally, the inhibition of rat Nav1.4 sodium channels expressed in oocytes by DCJW and RH4321 is also voltage-dependent (Silver and Soderlund, 2005a,b).

The results obtained in this study confirm that the action of DCJW is similar to that of RH3421, an earlier dihydropyrazole compound discovered by Rohm and Haas Co. (Salgado, 1992). Like DCJW, RH3421 did not block sodium channels (in crayfish giant axons) at the resting state, and a sustained depolarization up to a few seconds was necessary for RH3421 to achieve significant binding and inhibition. In this study, DCJW did not alter fast

inactivation or recovery from fast inactivation. However, because DCJW is slow-acting, the 200 ms depolarization used in the fast-inactivation recording protocol might not be long enough for the toxin to bind to sodium channels. Therefore, the slow action kinetics of DCJW limit the experimental assessment of state-dependent action of DCJW to mainly the slow-inactivated and resting states, but not the fast-inactivated state. The state-dependent block of sodium channels by RH3421 (Salgado, 1992) and DCJW (Zhao et al., 2003, 2005 and in this study) is reminiscent of the action of local anesthetics (e.g., lidocaine), which inhibit mammalian sodium channels in a state-dependent manner with a preference to the fast-inactivated state. However, RH3421 and DCJW bind to sodium channels much more slowly than lidocaine, so that the use-dependent block, a typical effect of local anesthetics, is not observed for RH3421 and DCJW.

The differential responses of two cockroach sodium channel variants, $BgNa_v1$-1 and $BgNa_v1$-4, to DCJW are intriguing. A recent study shows that neurons isolated from the CNS of the cockroach *P. americana*, contain two types of sodium currents, also differing in the voltage dependence of inactivation, and this difference was likewise shown to account for the differential sensitivity to DCJW (Zhao et al., 2005). The molecular basis of these two sodium currents remains to be determined, but it seems likely they are produced from two different sodium channel variants, similar to $BgNa_v1$-1 and $BgNa_v1$-4 identified in our study.

The present study also demonstrated the role of positively charged residues in IVS4 in the fast- and slow-inactivation of sodium channels. We show that the $BgNa_v1$-4 channel inactivates (both fast- and slow-inactivation) at more negative membrane potentials compared with $BgNa_v1$-1. Remarkably, substitution of the E residue in $BgNa_v1$-4 by a K is sufficient to produce a recombinant channel with voltage-dependence of fast- and slow-inactivation and DCJW sensitivity almost identical to those of the $BgNa_v1$-1 channel. Interestingly, the E1689K substitution does not alter the voltage-dependence of activation, in which $BgNa_v1$-1 and $BgNa_v1$-4 also differ significantly. Therefore, K1689E is involved specifically in modulating the voltage-dependence of fast and slow inactivation, and the voltage-dependence of fast-and slow-inactivation is a key determinant of DCJW sensitivity.

Acknowledgments

The work was supported by National Institutes of Health Grant GM057440 (to K.D.).

We thank Drs. Vincent Salgado and Kris Silver for critical review of this manuscript and Dr. Keith Wing for providing indoxacarb and DCJW for our study.

References

Catterall WA. From ionic currents to molecular mechanisms: the structure and function of voltage-gated sodium channels. Neuron 2000;26:13–25. [PubMed: 10798388]

Feng G, Deak P, Chopra M, Hall LM. Cloning and functional analysis of TipE, a novel membrane protein that enhances Drosophila Para sodium channel function. Cell 1995;82:1001–11. [PubMed: 7553842]

Hayward LJ, Brown RH Jr, Cannon SC. Slow inactivation differs among mutant Na channels associated with myotonia and periodic paralysis. Biophys J 1997;72:1204–19. [PubMed: 9138567]

Kuo CC, Bean BP. Slow binding of phenytoin to inactivated sodium channels in rat hippocampal neurons. Mol Pharmacol 1994;46:716–25. [PubMed: 7969051]

Lapied B, Grolleau F, Sattelle DB. Indoxcarb, an oxadiazine insecticide, blocks insect neuronal sodium channels. Br J Pharmacol 2001;132:587–95. [PubMed: 11159709]

Liu Z, Song W, Dong K. Persistent TTX-sensitive sodium current resulting from U-to-C RNA editing of an insect sodium channel. Proc Natl Acad Sci USA 2004;101:11862–7. [PubMed: 15280550]

Loughney K, Kreber R, Ganetzky B. Molecular analysis of the para locus, a sodium channel gene in Drosophila. Cell 1989;58:1143–54. [PubMed: 2550145]

Nagata K, Ikeda T, Honda H, Shono T. Suppression of voltage-gated sodium currents by the dihydropyrazole insecticide, DPX-JW062 in rat dorsal root ganglion neurons. J Pestic Sci 1998;23:62–4.

Narahashi T. Neuroreceptors and ion channels as the basis for drug action: past, present, and future. J Pharmacol Exp Ther 2000;294:1–26. [PubMed: 10871290]

O'Reilly JP, Wang SY, Wang GK. Residue-specific effects on slow inactivation at V787 in D2-S6 of Na(v) 1.4 sodium channels. Biophys J 2001;81:2100–11. [PubMed: 11566781]

Rudy B. Slow inactivation of the sodium conductance in squid giant axons: pronase resistance. J Physiol 1978;283:1–21. [PubMed: 722569]

Ruff RL, Simoncini L, Stuűhmer W. Slow sodium channel inactivation in mammalian muscle: a possible role in regulating excitability. Muscle Nerve 1988;11:502–10. [PubMed: 2453799]

Salgado VL. Slow voltage-dependent block of sodium channels in crayfish nerve by dihydropyrazole insecticides. Mol Pharmacol 1992;41:120–6. [PubMed: 1310138]

Schauf CL, Pencek TL, Davis FA. Slow sodium channel inactivation in Myxicola axons: evidence for a second inactive state. Biophys J 1976;16:771–8. [PubMed: 938717]

Silver KS, Soderlund DM. Action of pyrazoline-type insecticides at neuronal target sites. Pestic Biochem Physiol 2005a;81:136–43.

Silver KS, Soderlund DM. State-dependent block of rat $Na_v1.4$ sodium channels expressed in Xenopus oocytes by pyrazoline-like insecticides. Neurotoxicology 2005b;26:397–405. [PubMed: 15935211]

Simoncini L, Stuűhmer W. Slow sodium channel inactivation in rat fast-twitch muscle. J Physiol (Lond) 1987;383:327–37. [PubMed: 2443649]

Soderlund DM, Knipple DC. The molecular biology of knockdown resistance to pyrethroid insecticides. Insect Biochem Mol Biol 2003;33:563–77. [PubMed: 12770575]

Song W, Liu Z, Tan J, Nomura Y, Dong K. RNA editing generates tissue-specific sodium channels with distinct gating properties. J Biol Chem 2004;279:32554–61. [PubMed: 15136570]

Tan J, Liu Z, Nomura Y, Goldin AL, Dong K. Alternative splicing of an insect sodium channel gene generates pharmacologically distinct sodium channels. J Neurosci 2002;22:5300–9. [PubMed: 12097481]

Wang SY, Wang GK. A mutation in segment I-S6 alters slow inactivation of sodium channels. Biophys J 1997;72:1633–40. [PubMed: 9083667]

Warmke JW, Reenan RAG, Wang P, Qian S, Arena JP, Wang J, et al. Functional expression of Drosophila para sodium channels: Modulation by the membrane protein tipE and toxin pharmacology. J Gen Physiol 1997;110:119–33. [PubMed: 9236205]

Wing KD, Schnee ME, Sacher M, Connair M. A novel oxadiazine insecticide is bioactivated in lepidopteran larvae. Arch Insect Biochem Physiol 1998;37:91–103.

Wing KD, Sacher M, Kagaya Y, Tsurubuchi Y, Mulderig L, Connair M, et al. Bioactivation and mode of action of the oxadiazine indoxacarb in insects. Crop Prot 2000;19:537–45.

Wing, KD.; Andaloro, JT.; McCann, SF.; Salgado, VL. Indoxacarb and the sodium channel blocker insecticides: chemistry, physiology and biology in insects.. In: Gilbert, LI.; Iatrou, K.; Gill, SS., editors. Comprehensive insect science vol 6 insect control. Elsevier B.V.; 2004. p. 30-53.

Yarov-Yarovoy, Brown V, Sharp J, Clare JJ, Scheuer T, Catterall WA. Molecular determinants of voltage-dependent gating and binding of pore-blocking drugs in transmembrane segment IIIS6 of the Na channel α subunit. J Biol Chem 2001;276:20–7. [PubMed: 11024055]

Zhao X, Ikeda T, Yeh JZ, Narahashi T. Voltage-dependent block of sodium channels in mammalian neurons by the oxadiazine insecticide indoxacarb and its metabolite DCJW. Neurotoxicology 2003;24:83–96. [PubMed: 12564385]

Zhao X, Ikeda T, Salgado VL, Yeh JZ, Narahashi T. Block of two types of sodium channels in cockroach neurons by indoxacarb insecticides. Neurotoxicology 2005;26:455–65. [PubMed: 15935215]

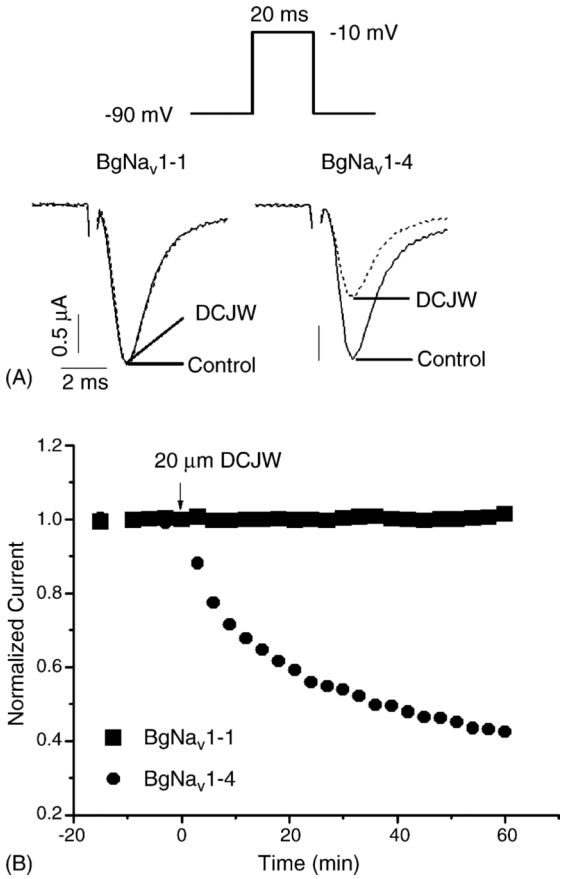

Fig. 1.

Effect of DCJW on the peak current of $BgNa_v1$-1 and $BgNa_v1$-4: (A) inhibition of the peak current of $BgNa_v1$-4 by DCJW (20 μM) and (B) time course of DCJW inhibition. The amplitude of the peak currents in the presence of DCJW was normalized to the peak current in control and plotted against the exposure time.

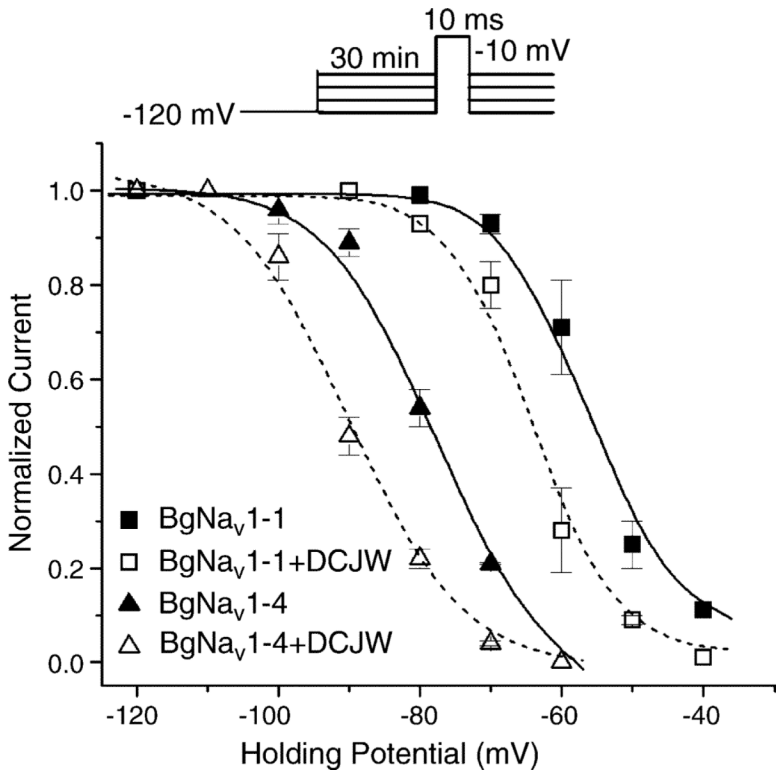

Fig. 2.

DCJW shifted the steady-state inactivation in the hyperpolarizing direction. For the control, peak current recorded at various holding potentials was normalized to the peak current recorded at the holding potential of −120 mV. For the DCJW treatment, peak currents recorded after 30 min of exposure to 20 μM DCJW at depolarizing holding potentials were normalized to the peak current at −120 mV in control. The data were fitted to the standard Boltzmann function. For BgNa$_v$1-4 in control: $V_{0.5}$ = −77.8 ± 0.9 mV, k = 6.5 ± 0.8, and treated with DCJW: $V_{0.5}$ = −90.0 ± 1.0 mV, k = 6.8 ± 1.0. For BgNa$_v$1-1 in control: $V_{0.5}$ = −56.5 ± 0.5 mV, k = 4.5 ± 0.4 and treated with DCJW: $V_{0.5}$ = −64.1 ± 0.9 mV, k = 4.3 ± 0.7. Each point represents data from four oocytes.

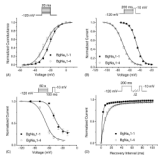

Fig. 3.

Gating properties of $BgNa_v1$-1, and $BgNa_v1$-4. (A) Normalized conductance curve. From the holding potential of −120 mV, currents (I_{Na}) were elicited by a 20 ms depolarization to varied potentials from −80 to 65 mV. Conductance (g) was calculated with equation $g = I_{Na}/(V - V_{rev})$, where V is the test pulse potential and V_{rev} is the measured reversal potential. (B) Voltage-dependence of fast inactivation. A 200 ms conditioning pulse to various potentials from −120 to 0 mV was followed by a 20 ms test pulse to −10 mV. Peak currents evoked by the test pulse were normalized to the maximum current and plotted against the conditioning potential. (C) Voltage-dependence of slow inactivation. A 60 s conditioning prepulse ranging from −120 to −20 mV was followed by a 100 ms interval at the holding potential of −120 mV and then a 10 ms test pulse to −10 mV to measure the available current. Peak current amplitudes of the test pulses were normalized to that obtained with a conditioning potential of −120 mV and plotted against the conditioning potentials. The lines in A–C were fits of data to standard Boltzmann function, and parameters were shown in Table 1. (D) Recovery from fast inactivation. After a 200 ms prepulse depolarization to −10 mV, the membrane potential returned to −120 mV for various periods of time, and a 20 ms test pulse to −10 mV was delivered to measure the available current. The peak current amplitude of test pulse was normalized to the peak current amplitude of the prepulse. Data were least-squares fitted with double exponential function: for $BgNa_v1$-1: τ_{fast} = 2.5 ms (89%) and for $BgNa_v1$-4: τ_{fast} = 8.5 ms (90%). Each point represents data from five to seven oocytes.

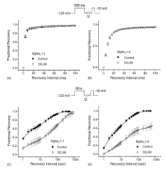

Fig. 4.

Effects of DCJW on recovery from fast inactivation and recovery from slow inactivation of $BgNa_v1$-1 (A and C) or $BgNa_v1$-4 (B and D). All data for DCJW were recorded after 30 min of DCJW (20 μM) treatment. (A and B) Recovery from fast inactivation. The protocol for recovery from fast inactivation was the same as those in Fig. 3. (C and D) Recovery from slow inactivation in the presence or absence of DCJW was measured using a 60 s depolarization to −10 mV followed by variable intervals at −120 mV and a subsequent 10 ms test pulse to −10 mV. The available current recorded with the test pulse was normalized to peak current recorded immediately prior to the recovery protocol. The lines are least-squares fits of double exponential function to the data. For $BgNa_v1$-1 in control: $\tau_1 = 1.1 \pm 0.1$ s (59%), $\tau_2 = 39 \pm 2$ s (41%); for $BgNa_v1$-1 exposed to DCJW: $\tau_1 = 4.5 \pm 0.2$ s (34%), $\tau_2 = 165 \pm 10$ s (66%); for $BgNa_v1$-4 in control: $\tau_1 = 2.3 \pm 0.2$ s (56%), $\tau_2 = 33 \pm 3$ s (44%); for $BgNa_v1$-4 exposed to DCJW: $\tau_1 = 14.9 \pm 1.0$ s (48%), $\tau_2 = 1572 \pm 200$ s (52%). Each point represents data from five oocytes.

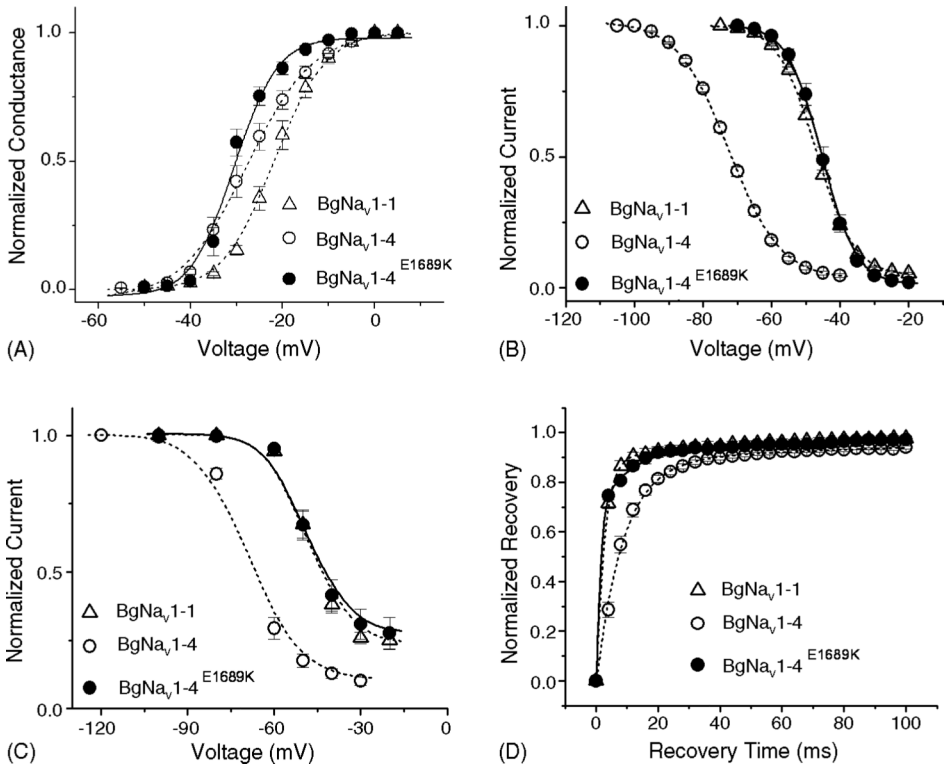

Fig. 5.

Gating properties of $BgNa_v1\text{-}4^{E1689K}$: (A) normalized conductance curve; (B) voltage-dependence of fast inactivation and (C) voltage-dependence of slow inactivation. The lines in A–C were fits of data to standard Boltzmann function, and parameters were shown in Table 1. (D) Recovery from fast inactivation. For $BgNa_v1\text{-}4^{E1689K}$: τ_{fast} = 1.5 ms (79%). The protocols were identical to those in Fig. 3. The gating properties of $BgNa_v1$-1 and $BgNa_v1$-4 from Fig. 3 are presented in dash lines for direct comparison. Each point represents data from four oocytes.

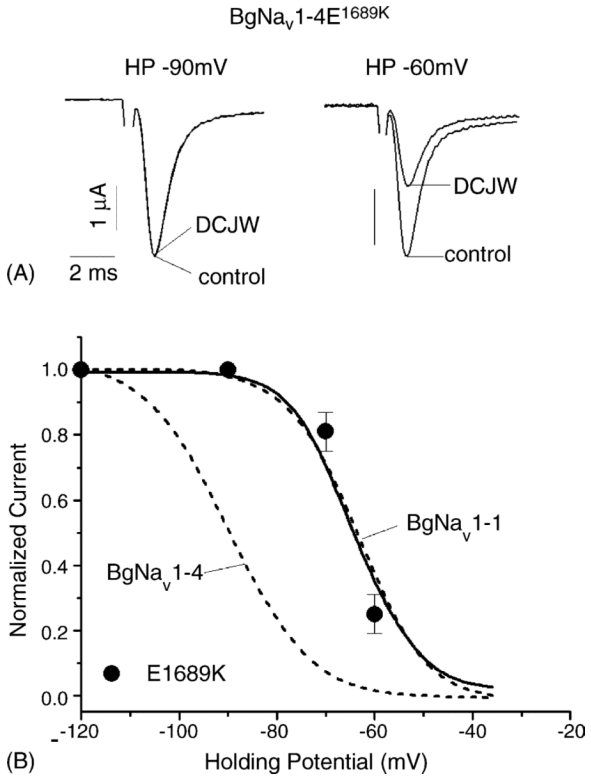

Fig. 6.

Inhibition of peak current of $BgNa_v1\text{-}4^{E1689K}$ by DCJW. (A) Sodium currents recorded by 20 ms depolarization to −10 mV from the holding potential of −90 or −60 mV in control or in the presence of DCJW (20 μM) for 30 min. (B) Voltage-dependence of DCJW inhibition. The protocols were the same as those in Fig. 2. Voltage-dependence of DCJW inhibition of $BgNa_v1\text{-}1$ and $BgNa_v1\text{-}4$ from Fig. 2 is indicated in dash lines for direct comparison. Each point represents data from four oocytes.

Table 1

Voltage-dependence of activation, fast inactivation, and slow inactivation of $BgNa_v1$-1, $BgNa_v1$-4 and $BgNa_v1$-4^{E1689K} channels

	Activation		Fast inactivation		Slow inactivation	
	$V_{0.5}$ (mV)	K	$V_{0.5}$ (mV)	K	$V_{0.5}$ (mV)	K
$BgNa_v1$-1	–21.7 ± 2.3	4.9 ± 0.7	–47.1 ± 0.8	5.1 ± 0.1	–48.5 ± 1.9	5.0 ± 0.7
$BgNa_v1$-4	–27.7 ± 3.9*	6.1 ± 0.4	–72.5 ± 1.3*	7.2 ± 0.2	–68.9 ± 1.1*	6.7 ± 0.5
$BgNa_v1$-4^{E1689K}	–30.4 ± 2.2*	3.4 ± 0.2	–45.5 ± 0.9	4.6 ± 0.2	–48.1 ± 0.9	5.2 ± 0.3

Data represent mean ± standard deviation for five to seven oocytes.

* $p < 0.05$ compared with $BgNa_V1$-1.

Neurotoxicology. Author manuscript; available in PMC 2011 March 15.